

QE
862
D5D4948
1990X
Vert. Pal.

Dinosaur Systematics

Approaches
and
Perspectives

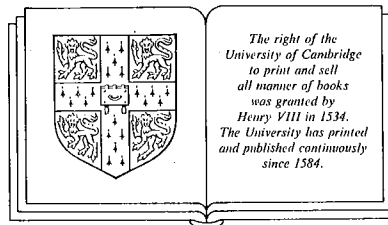
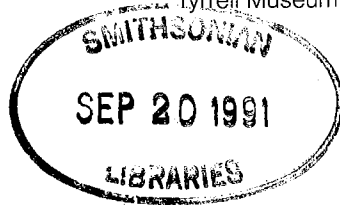
Edited by
Kenneth Carpenter

Denver Museum of Natural History

and

Philip J. Currie

Tyrrell Museum of Palaeontology



Cambridge University Press
Cambridge
New York Port Chester
Melbourne Sydney

12 Morphometric observations on hadrosaurid ornithopods

RALPH E. CHAPMAN AND
MICHAEL K. BRETT-SURMAN

Abstract

Results are presented of preliminary morphometric analyses on hadrosaurs using the landmark shape analysis method Resistant-Fit Theta-Rho-Analysis (RFTRA). The analyses were performed on both cranial and postcranial material. They show this approach to be useful for the analysis of hadrosaur morphology and provide insight into how this morphology varies within the context of the phylogenetic structure of the family. Further, the patterns are related to two other groups of Ornithopods, the iguanodontids and camptosaurids. The results highlight the distinct morphology of the lambeosaurine hadrosaurs, confirm that most of the significant morphological variation in hadrosaur crania is concentrated in the muzzle and nasal regions, and indicate that pelvic element shape should be useful for taxonomic identification and discrimination. In general cranial shape, the lambeosaurines are shown to be most closely related to the hadrosaurines, supporting a monophyletic Hadrosauridae.

Introduction

Hadrosaurs have one of the most complex taxonomic histories of all the dinosaurs; over 100 species representing 44 genera have been named. This unusually high taxonomic diversity is a consequence of the interplay between the taxonomic philosophies of the many researchers studying hadrosaurs, the high level of real taxonomic diversity, the unusually abundant material available, and the high degree of morphological variability within populations and between age groups. The latter is the result of allometric and ontogenetic effects over a wide range of sizes (see Dodson 1975; Hopson 1975; Molnar 1977). Herein, we will present the results of a series of preliminary shape analyses of hadrosaur crania and pelvis, and discuss these in the context of hadrosaur taxonomy, phylogeny, and identification.

Hadrosaurs are unusual among the dinosaurs

because they are represented by large numbers of well-documented specimens with both cranial and postcranial material. Contrast this with the pachycephalosaurs, for example, for which little postcranial material is available, and most taxa and specimens are represented by only incomplete crania (Maryańska and Osmólska 1974; Sues and Galton 1987; Goodwin this volume). In fact, hadrosaur material can be so abundant that it is often left uncollected when resources restrict the number of specimens that can be removed during a field season (P. Currie pers. comm. 1986).

In addition to this abundance, hadrosaurs exhibit a high degree of morphological variability, especially in cranial structures. These are thought by some to play a role in social behavior (Dodson 1975; Hopson 1975; Molnar 1977). Dodson (1975), for example, analyzed morphometric data for the crania of 36 specimens of lambeosaurine hadrosaurs referable to three genera (*Corythosaurus*, *Lambeosaurus*, and "*Procheneosaurus*") and 12 species. The approaches used included standard bivariate allometric analyses and principal coordinates analysis. Dodson concluded that the taxon "*Procheneosaurus*" includes only juvenile forms of other taxa, and that only one species of *Corythosaurus* and two of *Lambeosaurus* were represented, as well as both sexes. Clearly, the wide range of body size, the great diversity of display structures, and sexual dimorphism combined to produce a great deal of morphological variation among individuals of a single species.

The taxonomy of hadrosaurids has been the subject of discussion recently. Sereno (1986), in his cladistic analysis of the ornithischians, retained the hadrosaurs as a monophyletic taxon, whereas Horner (this volume) has suggested that the group is diphyletic.

Dinosaur morphometric analyses have been sporadic and limited by the small numbers of specimens available for most groups (Chapman this volume). The most comprehensive studies to date are Dodson's (1975)

work on lambeosaurine hadrosaurs, Dodson's (1976) allometric analysis of growth and sexual dimorphism in *Protoceratops*, the study of Chapman et al. (1981) on cranial allometry and sexual dimorphism in the pachycephalosaurian *Stegoceras*, the study of variation in *Plateosaurus* femora by Weishampel and Chapman (this volume), and the review by Chapman (this volume) demonstrating the application of shape analysis methods, specifically Resistant-Fit Theta-Rho-Analysis, to general problems of dinosaur paleobiology.

Generally, morphometric methods can provide important insights into the morphology of dinosaurs, and the implication of this morphology for interpreting phylogeny, ontogeny, paleoecology, and taphonomy. Morphometric methods already have provided important information on lambeosaurine variability (Dodson 1975). Here, we apply it more generally to hadrosaur morphology and to the interpretation of hadrosaur taxonomic structure.

Materials and methods

Resistant-Fit Theta-Rho-Analysis (RFTRA) is a form of landmark shape analysis that provides superimposed figures representing the fit of one specimen onto another after size and positional differences are removed, and gives distance values representing an estimate of the "goodness of fit." The fit is made using the relative positions of groups of landmarks (homologous or geometrically equivalent points) and the original geometry of the landmarks is maintained without the specimens being distorted during the analysis (Benson et al. 1982).

Landmark shape analysis methods are derived from the transformation grids developed by D'Arcy Thompson (1942), and include tensor methods (see Bookstein et al. 1985, and references therein) and vector methods (Sneath 1967). RFTRA was developed by Siegel and Benson (1982) and Benson et al. (1982), who modified Sneath's least-squares approach by applying more robust statistical methods (Siegel and Benson 1982). The RFTRA algorithm is a major improvement on the least-squares method (referred herein as LSTRA) because it allows localized change to be identified.

Chapman (this volume) presents a detailed discussion on the philosophy and mechanics of the method. In this study, a series of photographs/illustrations representing the same view was obtained for the specimens, and the questions to be addressed by this analysis were developed. Next, a series of homologous landmarks or equivalent points were located on each illustration. The resulting constellation of landmark points then was used to provide the fit of one specimen onto the base specimen. Each landmark had to be found on all specimens. A polygonal or "skeletal" diagram was developed that connected specified pairs of these landmarks representing functional units or individual skeletal elements. The RFTRA programs were then run on a computer to provide the necessary calculations, graphical output, and distance

coefficients (the estimate of the closeness of fit between the two specimens based on the superimposition).

The morphometric approaches used here were applied to provide insight into the morphology of the hadrosaurs and how the different hadrosaur morphologies interrelate. Iguanodontids were used as the primary outgroup to provide examples of the most closely related group to the hadrosaurs, and two specimens of camposaurids also were used as the second outgroup to give an indication of the morphological trajectory of the euornithopods (*sensu* Sereno 1986). A specimen of "*Procheneosaurus*," considered by us to be a juvenile lambeosaurine (fide Dodson 1975), was included to show how an immature form would compare with the adults, and whether it would cluster with the lambeosaurines.

One characteristic that morphometric analyses share with modern phylogenetic analyses is that they are both dialectic in nature: the results of an analysis are not considered to be the final answer but, instead, indicate the direction that further analyses should take. Because of this, we recognize these results as a first approach in the ongoing analysis of both cranial and postcranial elements of hadrosaurs and other euornithopods. The number of complete and articulated specimens available is exceedingly small. However, the results do indicate where expanded studies should concentrate.

The results of RFTRA within this context do provide information relevant to the interpretation of taxonomic and phylogenetic structure. If the results of a morphometric analysis do not agree with conventional phylogenetic reconstructions, then they raise questions that must be addressed before those phylogenies can be accepted. Often the differences can be recognized as convergence, providing information that may be relevant to the functional morphology or ecology of the taxon. Where convergence is not apparent, however, the characters used in the phylogenetic analysis should be reconsidered and additional morphometric analyses developed to try to reconcile the differences. Agreement between the two provides support in much the same way that the addition of new characters strengthens a phylogenetic analysis. It is more parsimonious to accept morphological similarity between the members of two groups as the result of recent ancestry rather than just a chance convergence, if other factors independently suggest the connection. In this way, morphometric analyses can help in the choice between two phylogenies developed using more conventional approaches.

In vertebrate paleontology, reconstructions such as those used for the analyses here represent the original skeletal material interpreted by paleontologists during the process of reconstruction. The results of morphometric analyses then provide a way to evaluate these interpretations within the context of those available for other related forms. As the resulting patterns are interpreted, they can suggest information that is relevant to the tax-

onomy and biology of the original animals, or they may suggest where the reconstruction process needs to be reconsidered (see example with *Protoceratops* in Chapman, this volume). In either case, the information is useful.

Two groups of analyses were done on specimens of hadrosaurids, including both hadrosaurines and lambeosaurines (Appendix 2), iguanodontids and *Camptosaurus*. The first analyses concentrated on illustrations of skulls, and used sutural connections of cranial bones, fenestrae, and geometrical points as landmarks. The specimens used and the source of the illustration are given in Table 12.1. Figure 12.1 shows representatives of the hadrosaurines and Figure 12.2 a lambeosaurine for comparison. An example illustrating the landmarks used and the resulting polygonal figure is shown in Figure 12.3.

The following 20 cranial landmarks were chosen as the most representative set to delineate the basic features of hadrosaur cranial morphology (see Figure 12.3). All points are those seen in lateral view.

1. The lateral interior inflection point of the premaxillary "lip."
2. The lateral exterior inflection point of the premaxillary "lip."
3. The medial exterior inflection point of the premaxillary "lip."
4. The medial interior inflection point of the premaxillary "lip."
5. The contact between the dorsal ramus of the premaxilla and the nasal.
6. The posterior limit of the true external narial opening.
7. The most posterior extent of the lower ramus of the premaxilla.
8. The posterior limit of the nasal (nasal/frontal contact in most cases).
9. Frontal/parietal contact.
10. The most dorsal extent of the lateral temporal fenestra.
11. The most anteroventral extent (inflection point) of the lateral temporal fenestra.
12. The most dorsal extent of the quadrate.
13. The ventral limit of the quadrate.
14. The superior jugal/quadratojugal/quadrato contact.
15. The inferior jugal/quadratojugal contact.
16. The posterior end of the maxillary dental battery.
17. The lacrimal/jugal/orbit contact.
19. The maxilla-lacrimal contact.
20. The anterior end of the maxillary dental battery.

Table 12.1. *Specimens/illustrations used for analysis of hadrosaur crania*

No. ^a	Taxon [Group] ^b	Source ^c
1	<i>Camptosaurus depressus</i> [C]	GAL, p. 82, Fig. 7A
2	<i>Iguanodon bernissartensis</i> [I]	OWN, Pl. 9, Fig. 1
3	<i>Ouranosaurus nigeriensis</i> [I]	TAQ, p. 62, Fig. 10A
4	<i>Edmontosaurus regalis</i> [H]	L&W, p. 152, Fig. 52
5	<i>Anatotitan copei</i> [H]	L&W, p. 158, Fig. 54
6	<i>Hadrosaurus notabilis</i> [H]	L&W, p. 167, Fig. 59
7	<i>Brachylophosaurus canadensis</i> [H]	HOLO., NMC 8893
8	<i>Maiasaura peeblesorum</i> [H]	HOR, p. 82
9	<i>Parasaurolophus maximus</i> [H]	L&W, p. 173, Fig. 63
10	<i>Saurolophus osborni</i> [H]	L&W, p. 176, Fig. 65
11	" <i>Procheneosaurus praeceps</i> " [L]	L&W, p. 181, Fig. 67
12	<i>Lambeosaurus lambei</i> [L]	L&W, p. 189, Fig. 72
13	<i>Lambeosaurus magnicristatus</i> [L]	L&W, p. 194, Fig. 76
14	<i>Corythosaurus casuarius</i> [L]	L&W, p. 196, Fig. 77
15	<i>Hypacrosaurus altispinus</i> [L]	L&W, p. 206, Fig. 86
16	<i>Parasaurolophus walkeri</i> [L]	L&W, p. 211, Fig. 89
17	<i>Corythosaurus excavatus</i> [L]	L&W, p. 198, Fig. 80
18	<i>Lambeosaurus lambei</i> [L]	L&W, p. 190, Fig. 73
19	<i>Corythosaurus intermedius</i> [L]	L&W, p. 200, Fig. 81
20	<i>Iguanodon atherfieldensis</i> [I]	ROM, p. 148, Fig. 79B

Note: ^aFor RFTRA specimen file numbers add 2000 to each number indicated. For example, cranial data for *Parasaurolophus walkeri*, #16, are contained in file #2016.

^b[C] = camptosaurid; [H] = hadrosaurine hadrosaur; [I] = iguanodontid; [L] = lambeosaurine hadrosaur

^cFig. = Figure; GAL = Galton 1980; HOLO. = Photograph of holotype; HOR = Horner and Gorman 1988; L&W = Lull and Wright 1942; NMC = National Museum of Canada; OWN = Owen 1855; p. = Page; Pl. = Plate; ROM = Romer 1956; TAQ = Taquet 1976.

The dentary and prementary were not used in this preliminary analysis because the latter is frequently lost. Many landmarks in an articulated dentary are hidden in lateral view.

These points were designed to highlight the four basic "taxonomic" skull sections when seen in lateral view. Each section displays its own unique attributes that have previously proven to contain most of the major morphological features used to delineate genera. Section 1 contains the reflected margin of the premaxilla, which in hadrosaurines forms the "lips." This area is especially important in the edmontosaur clade (Brett-Surman 1988) that contains *Edmontosaurus* (= *Anato-*

saurus), *Shantungosaurus*, and *Anatotitan* (Appendices 1 and 2). This area is represented by landmarks one through four. Section 2 is the most important area of analysis for hadrosaurines, and contains the external nares and the external narial pockets that figure prominently in hadrosaurines such as *Edmontosaurus* and *Hadrosaurus* (= *Kritosaurus* fide Horner). The section is bordered anteriorly by the reflected premaxillary lips and posteriorly by the closure of the external narial opening. Section 3 includes the nasal-frontal complex and represents the most diagnostic area for all lambeosaurines. Section 4, containing the quadrate and temporal fenestrae, shows the least amount of evolutionary change from the standpoint of shape analysis.

A second group of analyses used individual pelvic elements. True homologous landmarks were more difficult to find on these elements and, as a result, we relied more on geometrically analogous points, reflecting inflection points that control the major elements of shape for each element (see Bookstein et al. 1985). For this reason, the results should be used more as an indicator of how well these elements can be used for taxonomic identification, which points are most relevant in shape-change, and the potential for developing further studies that may provide more direct phylogenetic input. The

Figure 12.1. A comparison of two hadrosaurines: **A**, *Edmontosaurus regalis* (type) and **B**, *Anatotitan copei* (type), drawn to the same quadrate height to minimize size differences. Drawings by Gregory S. Paul.

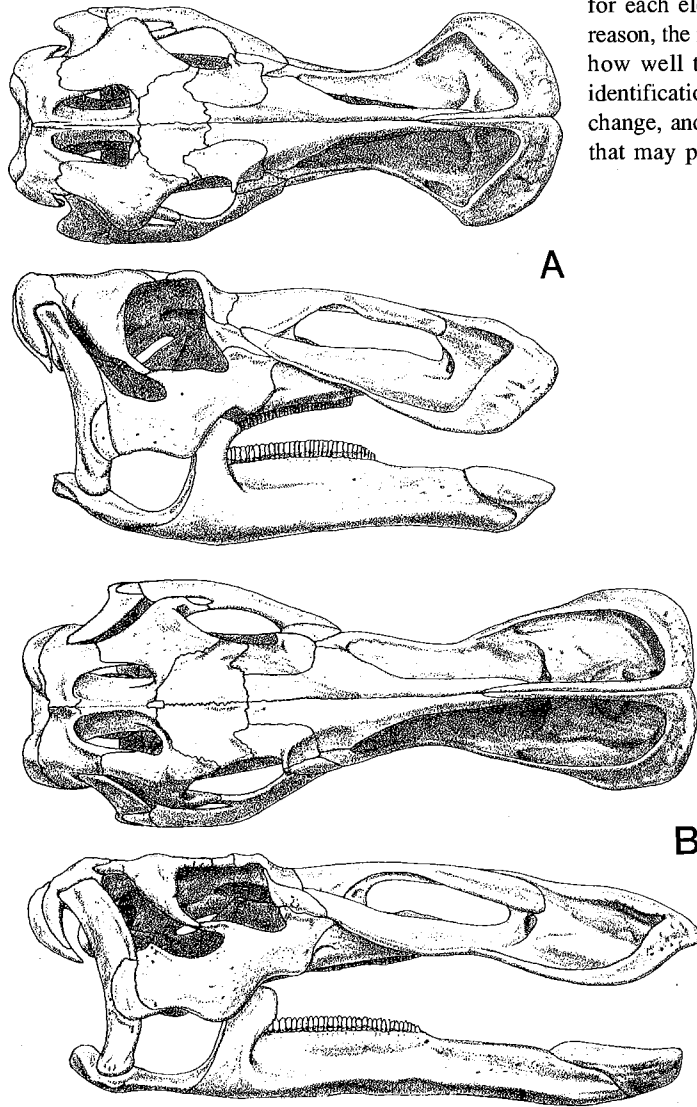


Figure 12.2. A skull of the lambeosaurine *Lambeosaurus lambei* (FMNH 1479). Compare with Figure 12.1. The main differences in shape between the two groups are concentrated in two bones, the premaxilla and the nasal. Although there are considerable shape differences in the premaxillary, there are few homologous points that can be discerned with accuracy. Most of the inflection points, dorsal limits, and projections are geographic points that are subject to intense ontogenetic allometry and thus are not as rigorously controlled as homologous points that can be precisely defined for the purposes of RFTRA.

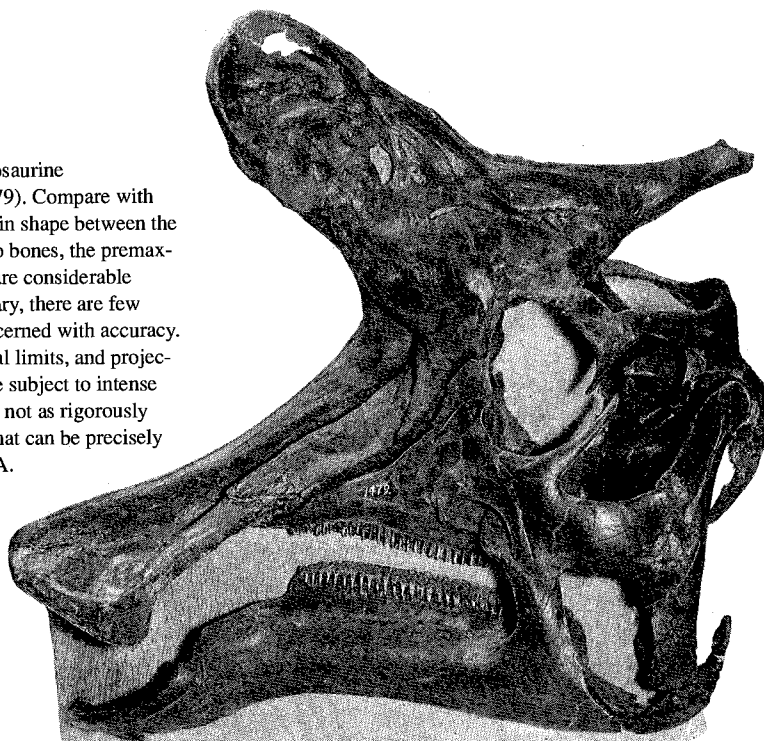
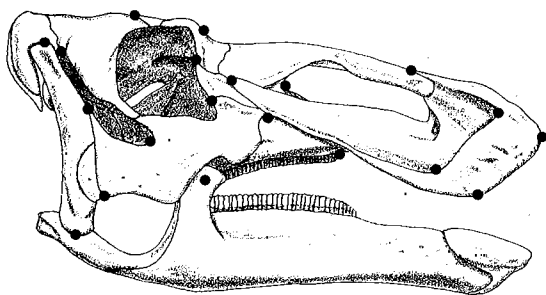
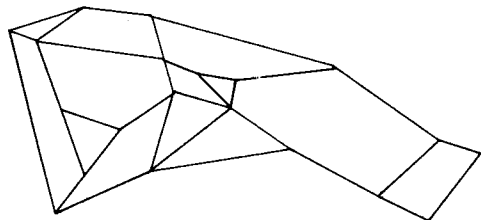


Figure 12.3. Landmarks and polygonal diagrams used for Resistant-Fit Theta-Rho-Analysis of cranial illustrations for hadrosaurids and advanced ornithopods. A, shows the illustration of *Edmontosaurus* from Figure 12.1 with the landmarks indicated by the black circles. B, gives an sample polygonal diagram of that specimen for use with RFTRA.



A



B

specimens used are given in Table 12.2, along with their current taxonomic assignment. Analyses were performed for specimens using the pubis, ilium, and ischium, the most diagnostic postcranial elements.

The landmarks used for the analysis of the pubis are illustrated in Figure 12.4A. The pubis is divided into three functional areas, the postpubis and acetabulum, the prepubic neck, and the expanded prepubic blade (Brett-Surman 1975, 1988). Each of these regions is represented by one or more polygons in the analyses. The true postpubis is vestigial and the ischial peduncle is relatively reduced. In each of the five main lineages of hadrosaurs (Brett-Surman 1979), the blade is the most important feature and is consistent in overall shape through time. In the transition from the hadrosaurine condition to that of the most advanced lambeosaurines (parasaurolaphs), there is a consistent shortening of the prepubic neck and an expansion (dorsoventrally) of the neck and blade.

The landmarks used for analysis of the ilium (Fig. 12.4C) were chosen to highlight the three functional/taxonomic sections of the hadrosaur ilium, each delimited by one or more polygons in the graphical output. They are:

1. The anterior limit of the preacetabular process.
2. The point halfway on the dorsal rim of the preacetabular process. The length of the preacetabular process is measured along the midline between perpendicular lines through the anterior tip of the process and the inflection point where the process meets the body of the ilium.

3. The most dorsal aspect of the iliac body and inflection point of the iliac rim above the pubic peduncle.
4. The anterior limit of the antitrochanter.
5. The most lateral extent and inflection point of the antitrochanter.
6. The posterior end of the antitrochanter.
7. The inflection point on the dorsal rim of the postacetabular process where it meets the antitrochanter.
8. The most posterior extension of the postacetabular process on its midline.
9. The ventral inflection point of the postacetabular process where it meets the body of the ilium.
10. The posterior node of the ischial peduncle.
11. The anterior node of the ischial peduncle.
12. The midline or inflection point of the acetabulum.
13. The node of the pubic peduncle.
14. The inflection point between the iliac body and the preacetabular process.
15. The ventral midline point of the preacetabular process.

The hadrosaur ilium is divided into three sections, each represented by one or more polygons in the graphics. The preacetabular process is, in most cases, a simple vertical bar that forms a shallow angle with the dorsal rim of the iliac body. In primitive hadrosaurs, this process is mostly straight and slightly deflected ventrally.

In advanced hadrosaurs, this process becomes strongly deflected, especially in *Hadrosaurus*. In old hadrosaurs that display hyperostosis, this process becomes T-shaped in cross-section and deepens. Lambeosaurine ilia are, in general, thicker and more robust than those in hadrosaurines.

The second major iliac section is represented by the body of the ilium, and contains the peduncles, antitrochanter, and the acetabulum. One major distinctive feature of the hadrosaurs, compared to the iguanodontid sister-group, is the large antitrochanter. This process only becomes relatively large in Campanian and Maastrichtian forms, and demonstrates the increasing importance of the pelvic-femoral protractors and retractors. In lambeosaurines, the body of the ilium is relatively taller than in the hadrosaurines.

The most highly evolved section of the hadrosaur ilium is the postacetabular process, which is greatly increased in length compared with iguanodontids. In lambeosaurines, this process is not as lengthy as in the hadrosaurines, but is much thicker and taller. In pre-Santonian hadrosaurs (*Secernosaurus* and *Gilmoresaurus*), this process is dorso-medially twisted and asym-

Table I2.2. *Specimens/illustrations used for analysis of hadrosaur pelves*

No. ^a	Taxon [Group] ^b	Elements ^c	Source ^d
1	<i>Parasaurolophus</i> [L]	PU, IL, IS	B-S
2	<i>Lambeosaurus</i> [L]	PU, IL, IS	B-S
3	<i>Saurolophus</i> [H]	PU	B-S
4	<i>Hadrosaurus</i> [H]	PU, IL, IS	B-S
5	<i>Edmontosaurus</i> [H]	PU, IL	B-S
6	<i>Camptosaurus</i> [C]	PU, IL, IS	B-S
7	<i>Ouranosaurus</i> [I]	PU, IL, IS	TAQ
8	<i>Hypacrosaurus</i> [L]	PU, IL, IS	BRO
9	<i>Hadrosaurus</i> (2)? [H]	PU, IL, IS	PHO1
10	<i>Camptosaurus</i> (2) [C]	PU, IL, IS	GIL1
11	<i>Bactrosaurus</i> [I]	PU, IL, IS	GIL2
12	<i>Iguanodon</i> [I]	PU, IL, IS	OWN
13	<i>Muttaborrasaurus</i> [I]	PU, IL, IS	B&M
14	<i>Anatotitan</i> [H]	PU, IL, IS	PHO2
15	<i>Gilmoresaurus</i> [H]	IL, IS	B-S
16	<i>Shantungosaurus</i> [H]	IS	B-S

Notes: ^aFor RFTRA specimen file numbers add 1000 to each number indicated for the pubis, 1100 for the ischium, and 1200 for the ilium.

^b[C] = camptosaurid; [H] = hadrosaurine hadrosaur; [I] = iguanodontid; [L] = lambeosaurine hadrosaur.

^cIL = ilium; IS = ischium; PU = pubis.

^dAMNH = American Museum of Natural History; B&M = Bartholomai and Molnar 1981; B-S = Brett-Surman 1975; BRO = Brown 1913; GIL1 = Gilmore 1909; GIL2 = Gilmore 1933; OWN = Owen 1855; PHO1 = Photograph of specimen AMNH 5465; PHO2 = Photograph of specimen AMNH 5730; TAQ = Taquet 1976.

metrical in shape. In later hadrosaurs it becomes more vertical and more symmetric in shape.

The landmarks used for the analysis of the ischium are illustrated in Figure 12.4B. The ischium is divided into three sections, the head, shaft, and foot, all represented by one or more polygons in the graphics. There are three types of footed ischia in hadrosaurs, not two as commonly believed (Lull and Wright 1942). The first is the lambeosaurine condition with a fully formed, distally expanded foot. The second is the bulbous or partially formed foot found in the earliest hadrosaurs, such as *Gilmoresaurus* and *Bactrosaurus*. This is also seen in the iguanodontids, and is the ancestral condition for

hadrosaurs. The last, and most derived type, is the complete absence of a distal expansion, found only in the hadrosaurines.

Results of preliminary morphometric analyses

Morphometric analysis of crania

The results of the Resistant-Fit Theta-Rho-Analysis (RFTRA) of the cranial material listed in Table 12.1 are summarized in the dendrogram in Figure 12.5, and an example comparing two specimens is presented in Figure 12.6. The dendrogram exhibits two major clusters, one for the Lambeosaurinae and the other for the hadrosaurine, camptosaurid, and iguanodontid taxa. Within the latter cluster two subgroups are evident, the first including both *Iguanodon* specimens and *Camptosaurus*, and the other including all the hadrosaurines and *Ouranosaurus*.

In initial analyses, *Maiasaura*, based on the original reconstruction published in Horner (1983), clustered problematically with *Camptosaurus*. The cause of this is apparent upon examination of the type material for *Maiasaura*, which shows that reconstruction to be misleading due to the limited quality and amount of material available at that time. Using a new reconstruction published in Horner and Gorman (1988), based on additional material, *Maiasaura* clusters with the other hadrosaurines, as would be expected. This illustrates the need to evaluate the results of any quantitative analysis for possible outliers, and the capability of RFTRA to indi-

Figure 12.4. Drawings of the type pelvis of *Parasaurolophus cyrtocristatus* made from original photos. Included are A, the pubis; B, the ischium; and C, the ilium. Note the damaged acetabulum on the ilium. Black circles delineate the landmark points used in the RFTRA technique. Landmark point number is not included but can be deduced from the discussion in the text. Labels refer to major sections of the elements. In the top figure (pubis): 1. acetabulum; 2. iliac peduncle; 3. pre-pubic neck; and 4. pre-pubic blade. In the middle figure (ischium): 1. acetabulum; 2. iliac peduncle; 3. obturator notch; 4. shaft; 5. toe of the foot; 6. body of the foot; and 7. heel of the foot. In the bottom figure (ilium): 1. preacetabular process; 2. iliac body; 3. acetabulum; 4. antitrochanter; and 5. postacetabular process.

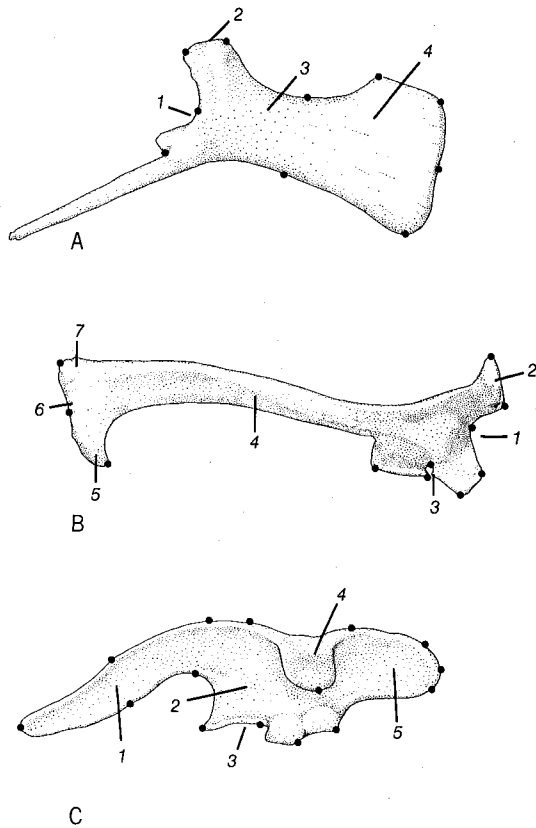
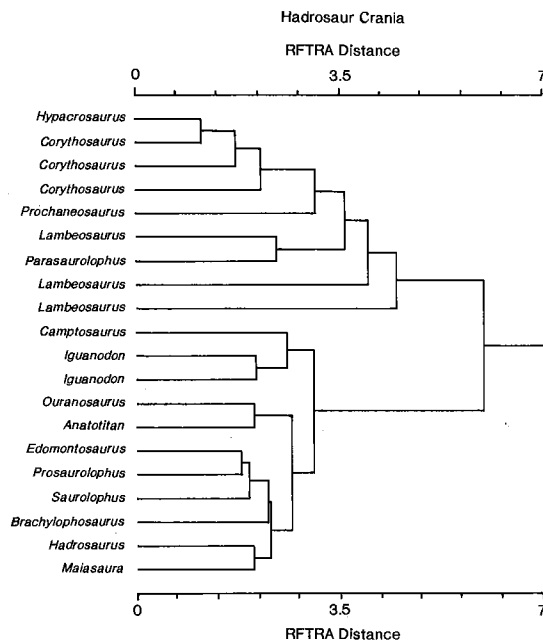


Figure 12.5. The dendrogram resulting from UPGMA cluster analysis of RFTRA distance coefficients for crania.

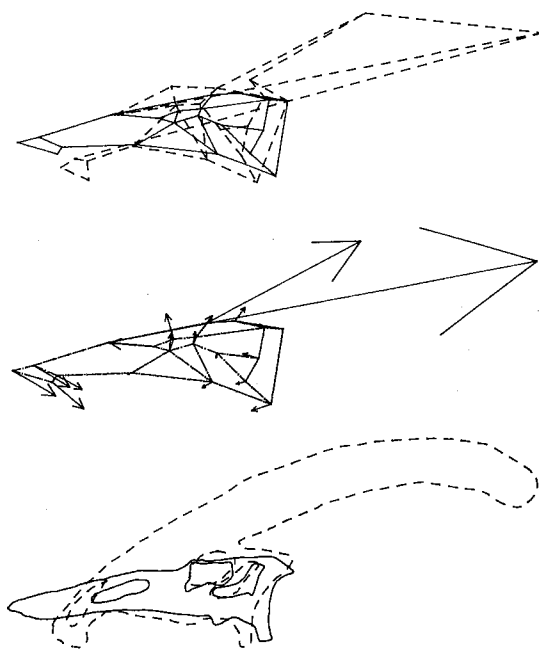


cate where possible problems occur in the data. The *Maiasaura* specimen does tend to have the highest similarity among the hadrosaurines with the iguanodontids and *Camptosaurus*, reflecting Horner and Gorman's (1988) suggestion that *Maiasaura* is an evolutionarily conservative "generalized hadrosaur" with close affinities to the iguanodontids.

The pairing of *Anatotitan* with *Ouranosaurus* is considered to be convergence. Both taxa have evolved independently towards an extremely elongate muzzle with an unexpanded narial opening.

The structure of the RFTRA distance matrix can be examined further by observing patterns in the average distance values within and among the major groups. The results are summarized in Table 12.3 for each comparison possible except for the camptosaurid-

Figure 12.6. Resistant-Fit Theta-Rho-Analysis of hadrosaurid crania. The top illustration provides superimposed polygonal diagrams, the middle figure a vector diagram of changes from the base specimen to the other, and the bottom figure superimposed outlines. Specimens 2005 (base) and 2016, $D = 13.2418$. Method = RFTRA, Skeleton = hadrosaur skull lateral. Specimen 2005 = *Anatotitan copei*. Specimen 2016 = *Parasaurolophus walkeri*. Figure 12.6 shows a comparison of a hadrosaurine (*Anatotitan*) to a lambeosaurine (*Corythosaurus casuarinus*). In actuality, the hadrosaurine skull is much longer than the lambeosaurine skull. RFTRA, however, shows that when absolute size is eliminated, the major differences are concentrated in the elaboration of the muzzle in hadrosaurines and the elaboration of the narial apparatus in lambeosaurines. Changes in the postorbital area are relatively minor.



camptosaurid pairing because there was only one specimen in that group. The data presented include mean values, standard deviations, and the number of total comparisons.

The results show that *Camptosaurus* has the highest similarity (= lowest RFTRA distance coefficients) with the iguanodontids and progressively lower similarities with the hadrosaurines and lambeosaurines. The lambeosaurines exhibit the opposite trend with the highest similarity with the hadrosaurines. The iguanodontids and hadrosaurines show a close affinity. Within-group comparisons show the highest average similarity within the hadrosaurines and the lowest in the lambeosaurines.

The largest RFTRA distance coefficient value, 8.129, is between *Lambeosaurus lambei* (reference #2018) and *Camptosaurus depressus* (2001). The lowest distance, 1.154, is between *Hypacrosaurus altispinus* (2015) and *Corythosaurus "intermedius"* (2019). Table 12.4 gives the mean RFTRA coefficient values and standard deviations for each specimen. The mean values range from low values of 3.803 for *Saurolophus* (2010) and 3.832 for "*Procheneosaurus*" (2011), to high values of 5.881, 5.680, and 5.270 for the specimens of *Lambeosaurus* (2018, 2013, and 2012) and 5.380 for *Parasaurolophus* (2016).

The second method for elucidating matrix structure is to perform a nearest-neighbor analysis, finding the specimen with the smallest distance (= highest similarity) for each specimen. Two approaches were used. In the first, the nearest-neighbor from among all the available specimens was found for each specimen. The results (Table 12.5) show that *Maiasaura* (2008) is the nearest-neighbor to *Camptosaurus*, although the two specimens of *Iguanodon* have just slightly higher distance values with *Camptosaurus*. The two specimens of *Iguanodon* are mutual nearest-neighbors. The only unexpected result is that *Anatotitan* served as the mutual nearest-neighbor for *Ouranosaurus* (2003), reflecting the convergence noted earlier. For the other specimens, hadrosaurines had hadrosaurine nearest-neighbors, and lambeosaurines had lambeosaurines.

The second approach used a modified nearest-neighbor analysis. Here, comparisons were made between the two major clusters apparent in the dendrogram (Fig. 12.7), the lambeosaurines and non-lambeosaurines. For each lambeosaurine, a nearest-neighbor was found from among the non-lambeosaurines. Conversely, a lambeosaurine nearest-neighbor was found for each non-lambeosaurine. The results were simple and unanimous. For lambeosaurine specimens, the hadrosaurine *Saurolophus* is always the nearest-neighbor. For all non-lambeosaurines, "*Procheneosaurus*" is the nearest-neighbor, usually by a wide margin.

A sample individual analysis (Fig. 12.6) shows a comparison of a hadrosaurine (*Anatotitan*) to a lambeo-

saurine (*Corythosaurus casuarius*). In reality, the hadrosaurine skull is absolutely much longer than the lambeosaurine skull. RFTRA, however, shows that when absolute size is eliminated, the major differences are in the muzzle in the narial apparatus. Changes in the post-orbital area are relatively minor.

Morphometric analysis of the pubis

The dendrogram resulting from the UPGMA cluster analysis of RFTRA distance coefficients (Fig. 12.7) shows overall pubic shape to be quite useful for delimiting major taxa within the advanced ornithopods, and should be useful for identifying isolated elements to

Table 12.3. *Resistant-Fit Theta-Rho-Analysis distance coefficient values for major taxa using cranial data*

Groups used for comparison	Mean	S.D.	N
Camptosaurs-iguanodonts	2.710	0.220	3
Camptosaurs-hadrosaurines	3.231	0.493	7
Camptosaurs-lambeosaurines	6.750	0.913	9
Iguanodonts-iguanodonts	3.041	0.798	3
Iguanodonts-hadrosaurines	2.824	0.432	21
Iguanodonts-lambeosaurines	6.097	0.921	27
Hadrosaurines-hadrosaurines	2.282	0.347	21
Hadrosaurines-lambeosaurines	5.858	0.952	63
Lambeosaurines-lambeosaurines	3.492	1.046	36

Note: N = number of comparisons used for calculation of mean and standard deviation; S.D. = standard deviation.

Table 12.4. *Resistant-Fit Theta-Rho-Analysis distance coefficient data for specimens used for cranial analysis*

No.	Taxon [Group] ^a	Mean	S.D.
1	<i>Camptosaurus</i> [C]	4.816	2.010
2	<i>Iguanodon</i> [I]	4.395	1.863
3	<i>Ouranosaurus</i> [I]	4.253	1.624
4	<i>Edmontosaurus</i> [H]	4.092	1.954
5	<i>Anatotitan</i> [H]	4.532	2.108
6	<i>Hadrosaurus</i> [H]	4.158	1.922
7	<i>Brachylophosaurus</i> [H]	4.064	1.660
8	<i>Maiasaura</i> [H]	3.934	1.844
9	<i>Prosaurolophus</i> [H]	4.198	2.009
10	<i>Saurolophus</i> [H]	3.803	1.386
11	" <i>Procheneosaurus</i> " [L]	3.832	0.676
12	<i>Lambeosaurus</i> [L]	5.270	1.678
13	<i>Lambeosaurus</i> [L]	5.680	1.439
14	<i>Corythosaurus</i> [L]	4.850	1.693
15	<i>Hypacrosaurus</i> [L]	4.598	1.646
16	<i>Parasaurolophus</i> [L]	5.380	1.436
17	<i>Corythosaurus</i> [L]	4.284	1.364
18	<i>Lambeosaurus</i> [L]	5.881	1.459
19	<i>Corythosaurus</i> [L]	4.744	1.815
20	<i>Iguanodon</i> [I]	4.527	1.943

Note: S.D. = standard deviation.

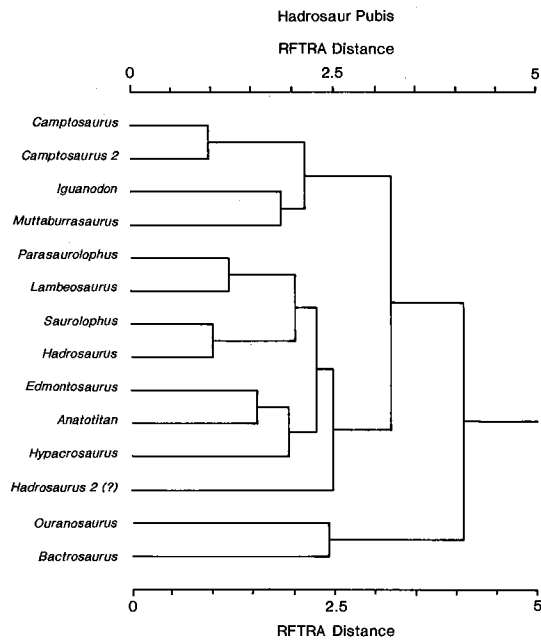
^a[C] = camptosaurid; [H] = hadrosaurine hadrosaur; [I] = iguanodontid; [L] = lambeosaurine hadrosaur.

Table 12.5. Nearest-neighbor data for cranial analyses using Resistant-Fit Theta-Rho-Analysis distance coefficients

Original Specimen		Nearest Neighbor		
No.	Taxon [Group] ^a	No.	Taxon [Group] ^a	Value
1	<i>Camptosaurus</i> [C]	8	<i>Maiasauria</i> [H]	2.513
2	<i>Iguanodon</i> [I]	20	<i>Iguanodon</i> [I]	2.051
3	<i>Ouranosaurus</i> [I]	5	<i>Anatotitan</i> [H]	2.020
4	<i>Edmontosaurus</i> [H]	6	<i>Prosaurolophus</i> [H]	1.801
5	<i>Anatotitan</i> [H]	3	<i>Ouranosaurus</i> [I]	2.020
6	<i>Hadrosaurus</i> [H]	4	<i>Edmontosaurus</i> [H]	1.919
7	<i>Brachylophosaurus</i> [H]	10	<i>Saurolophus</i> [H]	1.943
8	<i>Maiasaura</i> [H]	6	<i>Hadrosaurus</i> [H]	2.009
9	<i>Prosaurolophus</i> [H]	4	<i>Edmontosaurus</i> [H]	1.801
10	<i>Saurolophus</i> [H]	4	<i>Edmontosaurus</i> [H]	1.892
11	" <i>Procheneosaurus</i> " [L]	17	<i>Corythosaurus</i> [L]	2.532
12	<i>Lambeosaurus</i> [L]	16	<i>Parasaurolophus</i> [L]	2.422
13	<i>Lambeosaurus</i> [L]	12	<i>Lambeosaurus</i> [L]	3.747
14	<i>Corythosaurus</i> [L]	19	<i>Corythosaurus</i> [L]	1.522
15	<i>Hypacrosaurus</i> [L]	19	<i>Corythosaurus</i> [L]	1.154
16	<i>Parasaurolophus</i> [L]	12	<i>Lambeosaurus</i> [L]	2.422
17	<i>Corythosaurus</i> [L]	19	<i>Corythosaurus</i> [L]	2.011
18	<i>Lambeosaurus</i> [L]	19	<i>Corythosaurus</i> [L]	3.421
19	<i>Corythosaurus</i> [L]	15	<i>Hypacrosaurus</i> [L]	1.154
20	<i>Iguanodon</i> [I]	2	<i>Iguanodon</i> [I]	2.051

Note: ^a[C] = camptosaurid; [H] = hadrosaurine hadrosaur; [I] = iguanodontid; [L] = lambeosaurine hadrosaur.

Figure 12.7. A dendrogram resulting from the UPGMA cluster analysis of RFTRA distance coefficients for the pubis.



their correct taxon. The dendrogram shows two problematical outliers, *Ouranosaurus* and *Bactrosaurus*, that cluster together at a low level of similarity, suggesting unusual shapes for each and a small degree of convergence between the two taxa.

The other taxa fit nicely into the conventional phylogenetic structure accepted for advanced ornithomorphs. One major grouping clusters the hadrosaurids, and another the non-hadrosaurid taxa. Within the latter, the two specimens of *Camptosaurus* cluster together at a high level and the two remaining iguanodontids cluster together at a lower level, reflecting family level similarities. The hadrosaurid group includes a subcluster of two of the lambeosaurines, and others that give pairings of *Hadrosaurus* (= *Kritosaurus* following the classification given in Appendix 2) with *Saurolophus*, and *Edmontosaurus* with *Anatotitan*.

An example of the results from the individual comparisons is illustrated in Figure 12.8. Figures 12.8A-C demonstrate the shape changes from an iguanodontid (*Iguanodon*) to a hadrosaurid (*Parasaurolophus*). The results show that the acetabulum is enlarged, the prepubic neck and blade are enlarged, and that most of the changes are concentrated in the enlargement of the dorsal region of the blade.

Figures 12.8D-F demonstrates the changes of the pubis from a hadrosaurine (*Edmontosaurus*) to a lambeosaurine (*Parasaurolophus*). With the exception of the acetabulum, the same types of changes are seen as those from an iguanodontid to a hadrosaur, only to a smaller degree. In actuality, the hadrosaurine prepubis is absolutely much longer but the RFTRA technique reduced the elements to the same "best fit" to show true shape differences.

Morphometric analysis of the ilia

The dendrogram from analysis of the ilia is shown in Figure 12.9. The two specimens of *Camptosaurus* cluster together and with the iguanodontid *Muttaborrasaurus* at a low level of similarity, suggesting a high degree of variability in *Camptosaurus* and an ilium shape in those specimens distinct from that seen for the other taxa. Within the major cluster, including the iguanodontids and hadrosaurids, little structure of taxonomic interest is apparent, although *Edmontosaurus* and *Anatotitan* are joined with *Iguanodon*. In general, the dendrogram demonstrates the distinctiveness of the camptosaurids from the iguanodontids and hadrosaurids.

Figures 12.10A, B, C portray, as an example, the changes from an iguanodontid (*Iguanodon*) ilium to a hadrosaurid (*Parasaurolophus*) ilium. In hadrosaurs, the preacetabular process becomes longer and thicker, the acetabulum becomes deeper, the pubic peduncle is relatively reduced in size, and the postacetabular process

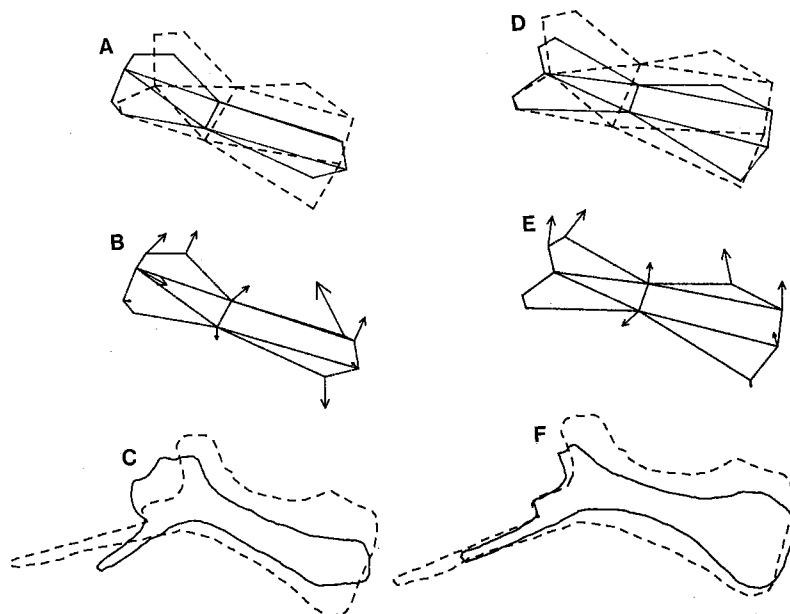
becomes more delineated from the body of the ilium as a separate feature (rather than an elongated posterior extension of the iliac body as in iguanodontids). This may be due to the increasing size and importance of the caudifemoralis musculature. The two largest changes are the increased height of the ilium and the tremendous increase in the size of the antitrochanter.

Figures 12.10D, E, F shows the shape change between a hadrosaurine (*Edmontosaurus*) and a lambeosaurine (*Parasaurolophus*) ilium. As before, the two major changes are the height of the iliac body and the relative increase of the antitrochanter.

Morphometric analysis of the ischia

The analysis of the ischia (Fig. 12.11) are the least useful taxonomically of all those presented, and suggest that either the ischium is of little use for taxonomic discrimination at the generic level, or that new analyses should be run using different landmarks. The connections appear to cut across recognized taxonomic lines except for the close pairing of the two specimens of *Camptosaurus*. Figure 12.12 compares a hadrosaurine (*Hadrosaurus*) ischium to a lambeosaurine (*Parasaurolophus*) ischium. In lambeosaurines, the iliac peduncle is enlarged and widened, and the ischial head is relatively larger. The greatest change is in the ischial foot. The increased thickness of the shaft is not shown here due to the lack of landmarks in this area.

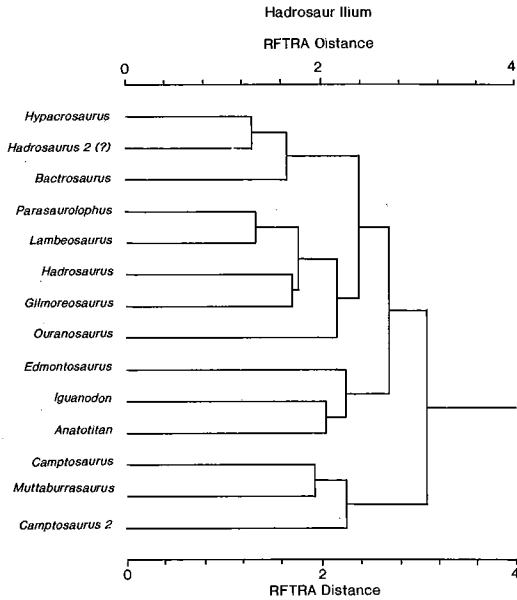
Figure 12.8. Results of a Resistant-Fit Theta-Rho-Analysis of the pubis for hadrosaurids and *Iguanodon*. Illustrations are as in Figure 12.6. A, B, C, demonstrate the shape changes from an iguanodontid (*Iguanodon*) to a hadrosaurid (*Parasaurolophus*). The RFTRA technique matches overall shape to a "best fit", consequently elements that are of different size are relatively reduced for the most accurate comparison. D, E, F, demonstrate the changes from a hadrosaurine (*Edmontosaurus*) to a lambeosaurine (*Parasaurolophus*).



Interpretation of morphometric analyses

The results of the morphometric analyses provide important insight into the morphological and possible phylogenetic relationships among the taxa studied. As

Figure 12.9. A dendrogram resulting from the UPGMA cluster analysis of RFTRA distance coefficients from the ilia.



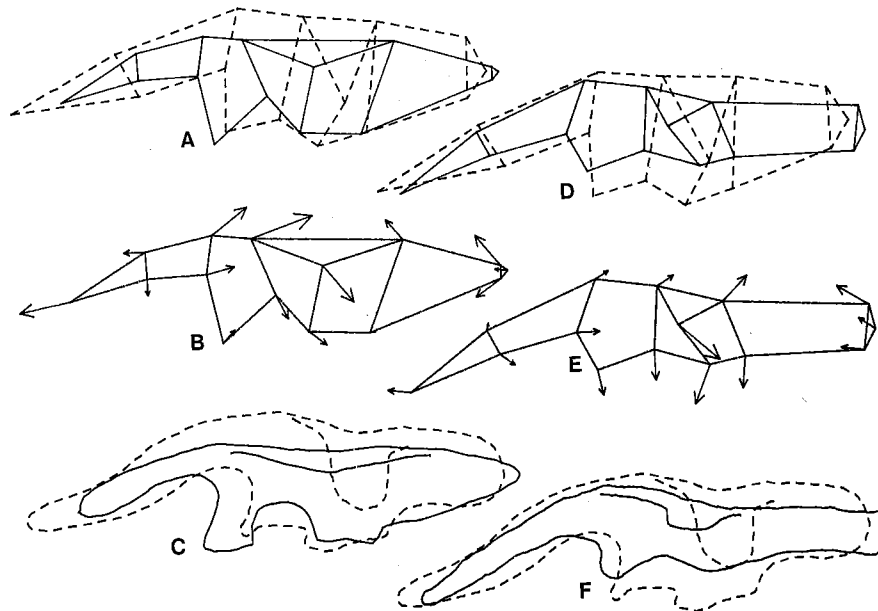
expected, cranial analyses provide the most insight, although analyses of the pelvic elements suggest that they have an excellent potential for the identification of suprageneric taxa among advanced ornithopods. At present, the types of landmarks used in the studies of the pelvic elements preclude making convincing statements in evaluating phylogenies except to support evidence derived from other analyses. However, the results suggest that useful insights may be obtained within this context if homologous points can be found on these elements and new RFTRA analyses run. This is an area of ongoing investigation (Brett-Surman and Chapman in progress).

The results of the cranial analysis (Fig. 12.5) strongly demonstrate the distinct nature of the lambeosaurines, especially considering the conservative nature of the landmarks chosen. Examination of individual comparisons confirms that the major differences between the hadrosaurines and the lambeosaurines are the result of changes mostly in the premaxillae and nasals.

The intergroup relationships among the non-lambeosaurines show that the groups are less distinct morphologically than are the lambeosaurines, but differences clearly are evident. The non-lambeosaurine sub-clusters separate the hadrosaurines from the iguanodontids and *Camptosaurus*, with the exception of the convergence of *Ouranosaurus* with the hadrosaurine *Anatotitan*.

The results of the cranial analysis suggest that the landmarks used are quite conservative among the

Figure 12.10. Results of a Resistant-Fit Theta-Rho-Analysis of ilia. Illustrations are as in Figure 12.6. A, B, C, portray the changes from an iguanodontid (*Iguanodon*) ilium to a hadrosaurid (*Parasaurolophus*) ilium. D, E, F, show the shape change between a hadrosaurine (*Edmontosaurus*) and a lambeosaurine (*Parasaurolophus*).



advanced ornithopods with moderate to small changes in position common even in the more distant pairings (e.g., *Camptosaurus* and *Parasaurolophus*). This is evidence for overall similarities in cranial morphology within the Euornithopoda. As would be expected from conventional taxonomic studies, the landmarks demonstrating the greatest changes, and thereby providing the greatest discrimination among taxa, are concentrated in the premaxillary lips, nasal area, and skull roof. The posteroventral landmarks tend to be far more conservative. The greater average distances among the lambeosaurines (Table 12.3) is to be expected due to high variability in forms thought to exhibit strong social behavior and sexual dimorphism (see Dodson 1975; Hopson 1975; Molnar 1977; Chapman et al. 1981).

The analyses run using pelvic elements, especially for the pubis, did provide additional insight into the relationships of the taxa studied. In general, the distinctness of the pelvic morphology of iguanodontids was clearly evident in all analyses. A close relationship between the lambeosaurines and hadrosaurines is evident in the analysis of the pubis, due to the presence only in hadrosaurids of a prepubic blade distinct from the prepubic neck.

Documenting whether the Hadrosauridae, including both the lambeosaurines and hadrosaurines, is monophyletic, as is accepted in most studies, or diphyletic, as suggested by Horner (this volume), is less straightforward. However, the analyses do provide important insights.

The average between-group RFTRA distance coefficients (Table 12.3) show that the lambeosaurines have the greatest average similarity with the hadrosaurines, the second greatest with the iguanodontids, and the least with *Camptosaurus*. This is as would be expected from published discussions (Lull and Wright 1942; Brett-Surman 1979; Sereno 1986) that assume monophyly. The relatively higher similarities among the non-lambeosaurines may appear to contradict this, but, instead, only indicate the high degree of morphological evolution within the lambeosaurine line. More relevant information is contained in the similarities of the lambeosaurines with all the other groups.

Powerful and supporting evidence comes from the second nearest-neighbor analysis between the lambeosaurine and non-lambeosaurine groups. If the lambeosaurines are derived from the iguanodontids independently from the hadrosaurines, then this analysis should have shown the lambeosaurines connecting preferentially to iguanodontids or, at the least, showing a

Figure 12.11. A dendrogram resulting from the UPGMA cluster analysis of RFTRA distance coefficients for the ischia.

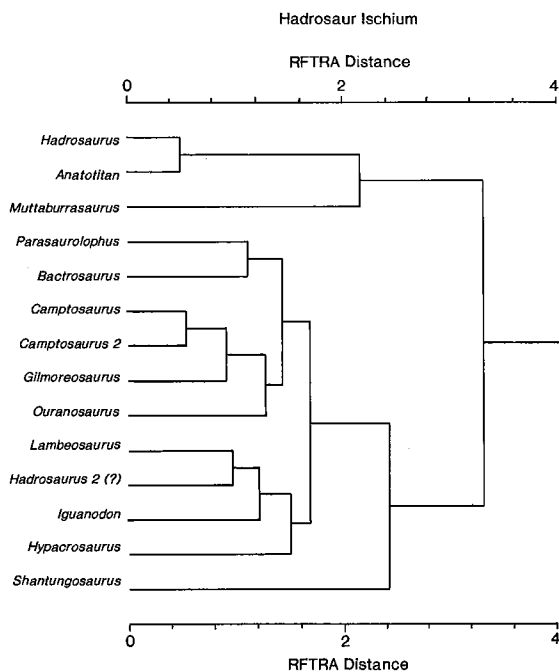
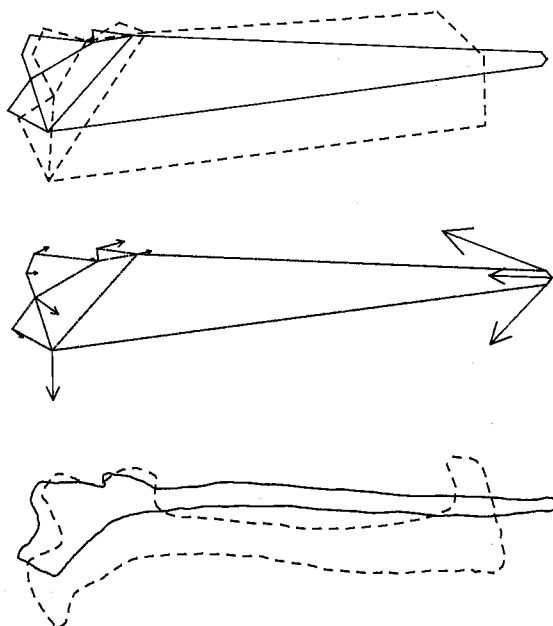


Figure 12.12. Results of a Resistant-Fit Theta-Rho Analysis of the ischium. Illustrations are as in Figure 12.6. Figure 12.12 compares a hadrosaurine (*Hadrosaurus*) ischium to a lambeosaurine (*Parasaurolophus*) ischium. In lambeosaurines, the iliac peduncle is enlarged and widened, and the ischial head is relatively larger. The increased thickness of the shaft is not shown here due to the lack of identifiable landmarks in this area. The greatest change is in the ischial foot. *Iguanodon*, *Bactrosaurus*, and *Gilmoreosaurus* all have an expanded bulb at the end of the ischium. Lambeosaurines have elaborated this condition in adults while juveniles still retain the plesiomorphic bulb. The synapomorphic condition is the loss of the distal ischial expansion found in all hadrosaurines.



wide variation. Instead, the lambeosaurines connect unanimously to the hadrosaurine *Saurolophus* and tend to have their lowest three to four distances with hadrosaurines. This, combined with recent phylogenetic analyses (e.g., Sereno 1986), strongly supports a close lambeosaurine-hadrosaurine link and argues convincingly for the Hadrosauridae as monophyletic. The less rigorously defined data for the pubis also supports a close lambeosaurine-hadrosaurine link, although far less convincingly.

Summary and conclusions

The hadrosaurids are a distinctive group of advanced ornithopods. The results of the morphometric analyses using the landmark shape analysis method Resistant-Fit Theta-Rho-Analysis (RFTRA) support a monophyletic interpretation for the Hadrosauridae.

Application of RFTRA to the crania of hadrosaurids, iguanodontids, and *Camptosaurus* provided important insights into morphological variability and taxonomic structure, and supports conventional phylogenetic interpretations of ornithopod phylogeny (e.g., Sereno 1986). Among hadrosaurids, most of the important morphological variability or evolution occurs in the muzzle and narial regions, providing the distinct cranial morphologies characterizing the hadrosaurid subfamilies (Figs. 12.1, 12.2).

Morphometric analyses using the pelvic elements were less successful because of the lack of homologous points and the use of geometrically defined points. However, the data did suggest strongly that element shape can be useful for the identification of taxa using isolated elements. For this study, the pubis provided the most information and the ilium, less. The ischium provided the least information, suggesting that it is not as diagnostic and that additional analyses need to be run (work in progress by the authors).

Acknowledgments

We would like to thank Linda Deck and Hans-Dieter Sues for reviewing our manuscript. We also would like to thank Phil Currie and Kenneth Carpenter for being understanding editors, and Jennifer Clark for providing us with illustrations despite our last minute requests. Special thanks to Gregory Paul for allowing us to use his restorations of *Edmontosaurus* and *Anatotitan*.

We wish to thank the following people for their help during the course of this study: Jose Bonaparte, Richard Fox, Phil Gingerich, James Jensen, Phil Currie, the late Ted White, the late Russell King, S. M. Kurzanov, Don Lindsey, Joanne Lindsey, the late Robert Makela, James Madsen, Christopher McGowan, William Morris, John Storer, William Turnbull, and the late C. C. Young.

Special thanks also are owed to David Berman, John Bolt, A. Gordon Edmund, Eugene Gaffney, Erle Kauffman, Harold E. Koerner, John Ostrom, Jane Danis, Dale Russell, Samuel P. Welles, Robert Purdy, Chip Clark, and Raymond Rye.

We are particularly indebted to the following individuals for their generous time and effort in aiding us during this study by providing data, equipment, photographs, helpful discussions, and active support: Don Baird, Alan Charig, John Horner, Joseph Gregory, Nicholas Hotton III, Douglas A. Lawson, Robert Long, David Norman, George Olshevsky, Halska Osmólska, Gregory S. Paul, Phillipe Taquet, Peter Galton, and John S. McIntosh.

References

- Bartholomai, A. and Molnar, R. E. 1981. *Muttaburrasaurus*, a new iguanodontid (Ornithischia: Ornithopoda) dinosaur from the Lower Cretaceous of Queensland. *Queensland Museum, Memoirs* 20(2):319-349.
- Benson, R. H., Chapman, R. E. and Siegel, A. F. 1982. On the measurement of morphology and its change. *Paleobiology* 8(4):328-339.
- Bookstein, F. L., Chernoff, B., Elder, R., Humphries, D., Smith, G. and Strauss, R. 1985. Morphometrics in evolutionary biology. *Academy of Natural Sciences, Philadelphia, Special Publications* no. 15:1-277.
- Brett-Surman, M. K. 1975. The appendicular anatomy of hadrosaurian dinosaurs. M.Sc. thesis (Berkeley: University of California).
1979. Phylogeny and paleobiogeography of Hadrosaurian dinosaurs. *Nature* 277(5697):560-562.
1988. Revision of the Hadrosauridae. Ph.D. thesis (Washington, D. C.: George Washington University).
- Brown, B. 1913. A new trachodont dinosaur *Hypacrosaurus* from the Edmonton Cretaceous of Alberta. *American Museum of Natural History Bulletin* 32(20):395-406.
- Chapman, R. E., Galton, P. M., Sepkoski, J. J. Jr., and Wall, W. P. 1981. A morphometric study of the cranium of the pachycephalosaurid dinosaur *Stegoceras*. *Journal of Paleontology* 55(3):608-618.
- Dodson, P. 1975. Taxonomic implications of relative growth in lambeosaurine dinosaurs. *Systematic Zoology* 24(1):37-54.
1976. Quantitative aspects of relative growth and sexual dimorphism in *Protoceratops*. *Journal of Paleontology* 50(5):929-940.
- Galton, P. M. 1980. European Jurassic ornithopod dinosaurs of the families Hypsilophodontidae and Camptosauridae. *Neues Jahrbuch für Geologie und Paläontologie, Abhandlungen* 160:73-95.
- Gilmore, C. W. 1909. Osteology of the Jurassic reptile *Camptosaurus*, with a view of the species and genus, and description of two new species. *United States National Museum, Proceedings* 36:197-332.
1933. On the dinosaurian fauna of the Iren Dabasu Formation. *American Museum of Natural History, Bulletin* 67(2):23-78.
- Hopson, J. A. 1975. The evolution of cranial display structures in hadrosaurian dinosaurs. *Paleobiology* 1(1):21-43.
- Horner, J. R. 1983. Cranial osteology and morphology of the type specimen of *Maiasaura peeblesorum* (Ornithischia: Reptilia) with a discussion of its phylogenetic position. *Journal of Vertebrate Paleontology* 3(1):29-38.

- Horner, J. R. and Gorman, J. 1988. *Digging Dinosaurs* (New York: Workman Publishing).
- Lull, R. S. and Wright, N. E. 1942. Hadrosaurian dinosaurs of North America. *Geological Society of America, Special Paper* no. 40:1-242.
- Maryńska, T. and Osmólska, H. 1974. Pachycephalosauria, a new suborder of Ornithischian dinosaurs. *Palaeontologia Polonica* 30:45-102.
- Molnar, R. E. 1977. Analogies in the evolution of combat and display structures in ornithopods and ungulates. *Evolutionary Theory* 3(3):165-190.
- Owen, R. 1855. Monograph on the fossil Reptilia of the Wealdon and Purbeck Formations. Part II. Dinosauria (*Iguanodon*) (Wealdon). *Palaeontographical Society, Monographs* no. 8:1-54.
- Romcr, A. S. 1956. *Osteology of the Reptiles* (Chicago: University of Chicago Press).
- Sereno, P. C. 1986. Phylogeny of the bird-hipped dinosaurs (order Ornithischia). *National Geographic Research* 2(2):234-256.
- Siegel, A. F., and Benson, R. H. 1982. A robust comparison of biological shapes. *Biometrics* 38:341-350.
- Sneath, P. H. A. 1967. Trend-surface analysis of transformation grids. *Journal of Zoology* 151:65-122.
- Sues, H.-D. and Galton, P. M. 1987. Anatomy and classification of the North American Pachycephalosauria (Dinosauria: Ornithischia). *Palaeontographica A*, 198:1-40.
- Taquet, P. 1976. *Géologie et Paléontologie du Gisement de Gadoufaoua (Aptien du Niger)* (Paris: Centre National de la Recherche Scientifique), pp. 1-191.
- Thompson, D. W. 1942. *On Growth and Form* (2nd edn.), vol. 1, 2 (Cambridge: Cambridge University Press).

Appendix 1

The diagnosis for *Anatotitan* is given below.

- Family Hadrosauridae
 Subfamily Hadrosaurinae
Anatotitan Brett-Surman, new genus
A. copei (Lull and Wright 1942) new combination
 Holotype: AMNH 5730
 Referred: AMNH 5886, 5887, CM 16520, and a mounted specimen in the Ekalaka Museum, Montana.
 Type locality: Near Moreau River, Black Hills, S. Dakota
 Age: Late Cretaceous, Maastrichtian
 Horizon: Hell Creek Formation
 Etymology: *Anas* (Latin: duck) and *Titan* (Greek: "large")

Diagnosis: Skull longer and lower than in any other hadrosaur, muzzle wider than in any other hadrosaur, quadrate/mandible ratio the smallest of all hadrosaurs, edentulous portion of the mandible relatively longer than in any hadrosaur, appendicular elements relatively longer and more gracile than in any hadrosaur of the same quadrate height, limb elements up to 10% longer than in an *Edmontosaurus* of the same quadrate height, neck of prepubis relatively longer and shallower than in any hadrosaur, postacetabular process more dorso-medially twisted and relatively shorter than in an *Edmontosaurus* of the same size.

Appendix 2

The following classification was used in this paper. Clade definitions and discussion are given in Brett-Surman (1988).

- Class Reptilia
 Subclass Archosauria
 Order Ornithischia
 Suborder Ornithopoda
 Infraorder Iguanodontia
 Family Hadrosauridae
 Subfamily Hadrosaurinae
 (edmontosaur clade) *Anatotitan*, *Edmontosaurus*, *Shantungosaurus*, *Tanius*, *Telmatosaurus* (= *Orthomerus*)
 (hadrosaur clade) *Aralosaurus*, *Brachylophosaurus*, *Hadrosaurus* (= *Kritosaurus* fide Horner, and *Gryposaurus*)
 (sauroloph clade) *Lophorhynchus*, *Maiaosaurus*, *Prosaurolophus*, *Saurolophus*
 Hadrosaurinae *incertae sedis*: *Secernosaurus*, *Gilmoreosaurus*
 Subfamily Lambeosaurinae
 (corythosaur clade) *Corythosaurus*, *Hypacrosaurus*, *Lambeosaurus*, *Nipponosaurus* (specimens assigned to "*Procheneosaurus*" are assumed to be juvenile members of this clade)
 (parasauroloph clade) *Bactrosaurus*, *Parasaurolophus*, *Tsintaosaurus*
 Lambeosaurinae *incertae sedis*: *Barsboldia*, *Jaxartosaurus*
 Hadrosauridae *incertae sedis*: *Mandschurosaurus*, *Cionodon*, *Hypsibema*, *Microhadrosaurus*, *Ornithotarsus*, *Pneumatoarthrus*
 Ceratopsia occasionally referred to the Hadrosauridae: "*Agathaumas*," *Claorhynchus*, (?)*Notoceratops*, (?)*Arstano-saurus*